UDK 621.777:539.92
Original scientific article/Izvirni znanstveni članek

ISSN 1580-2949
MTAEC9, 48(4)459(2014)

OPTIMIZATION OF THE MECHANICAL AND TRIBOLOGICAL PROPERTIES OF EXTRUDED AMCs: EXTENSION OF THE ALGORITHM SEARCHING AREA VIA MULTI-STRATEGIES

OPTIMIZACIJA MEHANSKIH IN TRIBOLOŠKIH LASTNOSTI EKSTRUDIRANIH AMC: RAZŠIRITEV ALGORITMA ISKALNEGA PODROČJA Z UPORABO VEČ STRATEGIJ

Mohsen Ostad Shabani, Ali Asghar Tofigh, Mohammad Reza Rahimipour, Mansour Razavi, Ali Mazahery, Fatemeh Heydari

Materials and Energy Research Center (MERC), Tehran, Iran
aliasghartofigh60@gmail.com

Prejem rokopisa – received: 2013-01-14; sprejem za objavo – accepted for publication: 2013-10-24

The present article focuses on the development of a comprehensive method for the optimization of the mechanical and tribological properties of metal-matrix composites using multi-strategy ensemble particle-swarm optimization. An aluminum-alloy matrix reinforced with coated B_4C particles was used for the present study. The cohesion of the reinforcing ceramic particles represents a very important factor, which is mostly poor at temperatures near the melting point of aluminum and leads to the inferior mechanical and tribological properties of the developed aluminum matrix composites with a non -uniform distribution of the reinforcement. The main reason for coating the particles is to improve the bonding between the reinforcement and the molten alloy and thus to eliminate any interfacial reactions. The great enhancement in the strength values of the composites in this study can be ascribed to the effective load-bearing capacity of the disintegrated B_4C particles, which are adherently bonded to the matrix alloy. Homogeneity and a reduction in the particle size of the B_4C during the extrusion process is evidenced in the microstructural studies.

Keywords: tribological properties, particle, extrusion process

Članek je osredinjen na razvoj celovite metode za optimizacijo mehanskih in triboloških lastnosti kompozitov s kovinsko osnovo z uporabo optimizacije več strategij združevanja gruč delcev. Za študij je bila uporabljena Al-zlitina, ojačana z obloženimi delci B_4C. Kohezija oplaščenih keramičnih delcev za utrjevanje je pomembna: navadno je slaba pri temperaturah blizu tališča aluminija in povzroča slabše mehanske in tribološke lastnosti razvitega kompozita na osnovi Al z neenakomerno razporeditvijo delcev za ojačanje. Glavni namen oplaščenja delcev je izboljšanje povezave med delcem za ojačanje in staljeno zlitino ter odprava reakcij na površini stika. Veliko povečanje trdnosti kompozita v tej študiji se lahko pripiše učinkoviti nosilnosti razpadlih delcev B_4C, ki so adherentno vezani na osnovno zlitino. Študije mikrostrukture so pokazale homogenost in zmanjšanje delcev B_4C med iztiskovanjem.

Ključne besede: tribološke lastnosti, delec, postopek iztiskovanja

1 INTRODUCTION

The particle-swarm algorithm tries to simulate the social behavior of a population of agents or particles, in an attempt to optimally explore a given problem space.[1] At a time instant (an iteration in the optimization context), each particle is associated with a stochastic velocity vector, which indicates where the particle is moving to[2–5]. The velocity vector for a given particle at a given time is a linear stochastic combination of the velocity in the previous time instant, of the direction to the particle's best position, and of the direction to the best swarm positions (for all particles).[6] The particle-swarm algorithm is a stochastic algorithm in the sense that it relies on parameters drawn from random variables, and thus different runs for the same starting swarm may produce different outputs.[7] Some of its advantages are that it is simple to implement and easy to parallelize.[8,9] It depends, however, on a few of parameters that influence the rate of convergence in the vicinity of the global optimum.[10] Overall, it does not require many user-defined parameters, which is important for practitioners that are not familiar with optimization.[11–13] Some numerical evidence seems to show that a particle swarm can outperform genetic algorithms on difficult problem classes, i.e., for unconstrained global optimization problems. Moreover, it fits nicely into the pattern search framework.[14,15]

During the past decade, novel computational methods have been introduced in some fields of engineering sciences, including the solidification and deformation of metal-matrix composites in materials science.[16–18] Aluminum metal-matrix composites (AMCs) are gaining importance as the most sought-after candidate materials in the space and automotive industries owing to their excellent properties, such as superior wear resistance, low density and high specific stiffness.[19–32] Several reports have been published addressing the problems associated with their developments, mechanical behavior, microstructure and the distribution of particulates.[33–41] Presently, particulate-reinforced composites are being produced by several different methods: powder metallurgy, liquid metallurgy, diffusion bonding techniques, infiltration, squeeze casting, compocasting and spray deposition techniques.[42–48] The most simplified approach to develop near-net -shaped aluminum-based composites is by the liquid metallurgy route as it is economical and can result in mass production.[18–20] Generally, these composites consist of a metal matrix, which is melted during casting, and ceramic reinforcement, which is added to the molten matrix material by a mechanical stirrer. However, some challenges need to be addressed in the development of AMCs to intensify their uses in different engineering fields, including inferior bond and interfacial reaction product. These problems do have a direct deteriorating effect on the mechanical and tribological properties of the composites, making them unsuitable for industrial components.[3] These challenges have been addressed to by the use of coated reinforcement and the addition of reactive metals like magnesium by several researchers. In addition, instead of conventional stir-casting techniques, semi-solid agitation processes can be employed. The benefits include reduced solidification shrinkage, a lower tendency for hot tearing, suppression of segregation, settling or agglomeration and faster process cycles. These advantages are accompanied by a lack of superheat (lower operating temperatures) as well as a lower latent heat, which results in a longer die life together with a reduced chemical attack of the reinforcement by alloy, also a globular, non-dendritic structure of the solid phase, which then explains the thixotropic behavior of the material.[18–20] Furthermore, these compocast-coated composites can be subjected to secondary processing such as extrusion and forging to improvise upon the mechanical properties in particular strength coupled with practical ductility.[39–43] The purpose of this study is first to investigate the effects of extrusion and reinforcing coated particles on the microstructures and mechanical properties of AA6061 aluminum alloy matrix composites produced by compocasting. Another objective is to solve the global problems using Multi-strategy ensemble particle-swarm optimization, which helps to increase the possibility of industrial application.

2 EXPERIMENTAL PROCEDURE

In this study, composites were produced by the compocasting process using the mechanical mixing of the AA6061 aluminum matrix, i.e., B_4C particles. The AA6061 aluminum alloy was produced from the mass fraction w = 99.9 % pure aluminum that had been melted and then a pure silicon master alloy in mass fractions of Al–75 % Cr, Al–50 % Cu, and pure magnesium were added in order. Boron carbide (B_4C) in powder form is used as the reinforcement, having a particle range size of 1–60 µm. We attempted to coat the B_4C powders with TiB_2, which helps the incorporation of the particles and reduces interfacial reactions. Titanium tetraisopropoxide was selected as a sol-gel precursor and diluted with ethanol. The boron carbide powders were first dispersed in the ethanol using a stirrer and then titanium tetraisopropoxide and distilled water were added to the stirred suspension. The processing was conducted at room temperature at a solution pH of 7. The solution was then aged for 105 min at room temperature, with constant, gentle stirring. When titanium tetraisopropoxide is used as the precursor, TiO_2 can be produced by hydrolysis and heat treatment. Since titanium oxide does not support good wettability, it is converted to TiB_2. **Figure 1** presents the X-ray diffraction (XRD) analysis of the coated powders.

The composites were developed using the stir-cast method. The process involved melting the alloy in a graphite crucible using an electrical resistance furnace. The stirrer was positioned just below the surface of the slurry. The furnace is controlled using a J-type thermocouple located inside the gas chamber. The temperature of the alloy was raised to about 680 °C and stirred at (400, 500, 600, 700) r/min using an impeller fabricated from graphite and driven by a variable ac motor. The stirring times were noted at (5, 10 and 15) min after the addition of B_4C during the process. Both TiB_2 coated and uncoated boron carbide was varied in proportions of volume fractions (2.5, 5, 7.5, 10, 12.5, 15) %. The temperature of the furnace was gradually lowered until the melt reached a temperature in the liquid-solid state (corresponding to a 0.2 solid fraction) while the stirring was continued. The coated particles were added uniformly at a rate of 50 g/min over a time period of approximately 3 min. The casting was obtained by pouring the composite slurry into a steel die placed below the furnace. A continuous purge of nitrogen gas is used inside and outside the crucible to minimize the oxidation of the molten aluminum. The cast matrix alloy and the developed Al6061–B_4C composites (both uncoated and TiB_2 coated) were machined to 70 mm diameter and 200 mm length. The machined billets were then subjected to hot extrusion using a 200 t hydraulic extrusion press. The extrusion billets were heated in a muffle furnace for 2 h. An extrusion ratio of 1 : 10 with a constant ram velocity (extrusion speed) of 2 mm/s was implemented. The extruded Al6061 alloy and Al6061–B_4C composites (both

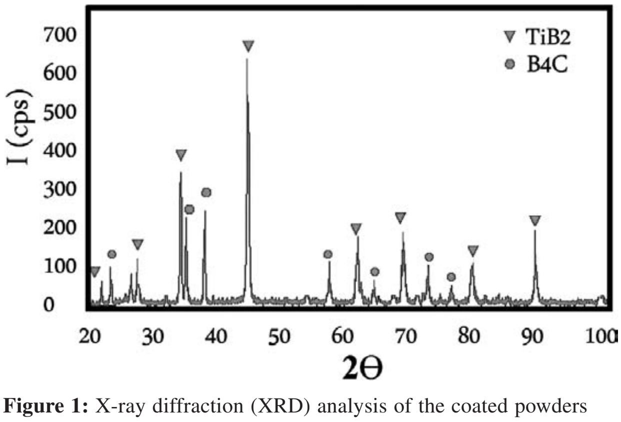

Figure 1: X-ray diffraction (XRD) analysis of the coated powders
Slika 1: Rentgenska difrakcijska analiza oplaščenega prahu

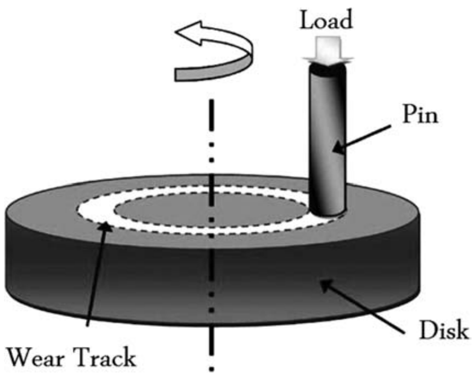

Figure 2: Schematic diagram of the abrasion wear test
Slika 2: Shematski prikaz preizkusa abrazijske obrabe

uncoated and TiB_2 coated) were subjected to metallographic studies, microhardness, tensile and wear tests.

Dry sliding wear tests were performed using pin-on-disk apparatus, under a load of 10 N and 20 N against a counterface steel disk of hardness 60 HRC. Cylindrical specimens of 6 mm diameter and 25 mm height were used as the test samples. Before the abrasion tests, each specimen was polished to 0.5 μm. **Figure 2** shows a schematic diagram of the abrasion wear test. The experiment was carried out at room temperature with water as the lubricant. The wear loss was measured in the steady-state regime using a linear variable differential transducer of accuracy 1 μm at the end of 30 min. The wear rates were calculated from height-loss data. A set of three samples was tested in every experimental condition, and the average along with the standard deviation for each set of three tests was measured. The wear tests were conducted up to the total sliding distance of 2000 m. The tensile test samples were machined according to the ASTM E8M standard. Hardness measurements were carried out using a Shimadzu Microhardness tester with a load of 1 N for a period of 10 s. For each sample, five hardness tests on randomly selected regions were performed in order to eliminate the possible segregation effects and obtain a representative value of the matrix material hardness. During the hardness measurements, precaution was taken to make an indentation at a distance of at least twice the diagonal length of the previous indention.

3 MODELING

3.1 Particle swarm optimization

The particle swarm optimization (PSO) was originally designed by Kennedy and Eberhart (Kennedy and Eberhart, 1995) and has been compared to genetic algorithms for efficiently seeking optimal or near-optimal solutions in large search spaces.[3] It is a new search technique, which simulates preying behavior among birds.[2] In contrast to genetic algorithms, PSO does not need genetic operations such as crossover and mutation. Instead, it changes the individuals by their random velocities in the solution space.[49–54] Compared to evolutionary algebra, the solution group presents greater randomness and more benefits, such as faster searching speed, easy implementation and global optimization.[3] In the original PSO with M particles, each particle is represented as a potential solution to a problem in a *D*-dimensional space and its position at the *t*-th iteration is denoted as:[1]

$$X_i = (x_{i1}^t, x_{i2}^t, x_{iD}^t) \tag{1}$$

Each particle remembers its own previous best position and its velocity along each dimension as:[49–52]

$$V_i = (v_{i1}^t, v_{i2}^t, v_{iD}^t) \tag{2}$$

The velocity and position of particle i at the $(t + 1)$th iteration are updated by the following equations:[3]

$$V_{i,j}^{t+1} = wV_{i,j}^t + c_1 r_{1i.j}^t (p_{ij}^t - x_{ij}^t) + c_2 r_{2i.j}^t (Q_j^t - X_{i,j}^t) \tag{3}$$

$$X_{i,j}^{t+1} = V_{i,j}^{t+1} + X_{i,j}^t \tag{4}$$

where c_1 and c_2 are two positive constants, known as the acceleration coefficients; r_1 and r_2 are two uniformly distributed random numbers on the range (0.1) for the j-th dimension of particle i. Vector $p_i = (p_{i1}^t, p_{i2}^t \ldots p_{iD}^t)$ is the position with the best fitness found so far for the ith particle, which is called the personal best (p_{best}) position. And vector $Q_i = (Q^t{}_1, p^t{}_2 \ldots p^t{}_D)$ records the best position discovered by the swarm so far, known as the global best (g_{best}) position. $x_{i,j}^t$, $v_{i,j}^t$ and $p_{i,j}^t$ are the jth dimension of the vector of $x_i{}^t$, $v_{i,}{}^t$ and $p_i{}^t$, respectively. The parameter w is the inertia weight used for the balance between the global and local search abilities. Usually, w decreases linearly with the iteration generations as:[1–4]

$$w = w_{max} - \frac{t(w_{max} - w_{min})}{T} \tag{5}$$

where w_{max} and w_{min} are the maximum and minimum weights and usually set to 0.9 and 0.4, respectively. T is a predefined maximum number of iterations, and t represents the number of the current iteration.

3.2 Multi-strategy ensemble particle swarm optimization (MEPSO)

In MEPSO, all the particles are initially divided into two parts; we denote them as part I and part II, respectively. The two parts are considered to play different roles in the search of dynamic environments by using different strategies, which will be introduced as follows. The role of part I is considered to search the global optimum in the current environment as quickly as possible. Thus, similar operations as the standard PSO are adopted to guarantee good convergence. Furthermore, a Gaussian local search is introduced to enhance the local search ability of part I, which is designed as follows:

At every iteration, for each particle, it has the probability P_{ls} to perform the Gaussian local search defined as Eqs. (4) and (6), and has the probability $(1 - P_{ls})$ to perform the conventional search defined as Eqs. (3) and (4). The global best used in part I is the best solution found by all particles, both in part I and part II. The Gaussian local search is defined as follows:

$$V_{i,j}^{t+1} = c_3 * \text{gaussrand} \tag{6}$$

where i = 1, 2, ... m, gaussrand is a random number generated from a standard normal distribution, c_3 is a positive constant. Although both strategies are designed for local search, the Gaussian local search adopted in part I of MEPSO is different from the quantum cloud defined in MQSO; the distribution in quantum cloud is uniform while Gaussian is not. The Gaussian local search strategy defined as Eq. (6) has been testified by many researches to be a good strategy to enhance the ability of elaborate search. By performing a local search with the probability P_{ls}, a particle can search for the optimum around its current position when it is on the process of "flying" to the best position found by the entire swarm.

Therefore, each particle has the chance to search for its neighborhood, and it might be favorable to find the optimum in dynamic multimodal environments. The role of part II is considered to extend the searching area of the algorithm, and to patrol around the part I to track the changed global optimum possibly "escaped" from the coverage of part I. To achieve this purpose, in part II, each particle has a probability 0.5 to fly to get closer to the personal best of a particle randomly chosen from part I, and has probability 0.5 to fly to get farther away from it. The operator is defined as Eq. (7), we call it differential mutation in this paper. It is implemented by changing the direction of a particle's velocity with a certain probability. The position of the particle is still renewed by Eq. (4):

$$\begin{aligned} V_{i,j}^{t+1} &= wV_{i,j}^{t}\,\text{sgn}(r_1-0.5)+c_1 r_{2i,j}^{t}(p_{ij}^{t}-x_{ij}^{t})+ \\ &+c_2 r_{3i,j}^{t}(G_j^{t}-X_{ij}^{t}) \end{aligned} \tag{7}$$

$$\text{sgn}=\begin{cases} -1 t<0 \\ 0 t=0 \\ 1 t>0 \end{cases} \tag{8}$$

where G_j is the best solution found by particle a, which is chosen randomly from part I at each iteration; r_1, r_2, r_3 are uniformly distributed random numbers in the interval (0, 1); other parameters are the same as the ones described in Section PSO. The strategy of differential mutation may enhance the communication between part I and part II, extend the particle's search area, and prevent the algorithm from being premature.

In part II, particles fly in a way totally different to the standard PSO. There is no global attractor in part II, the position of each particle in part II is determined by the particle in part I via differential mutation strategy (each particle has a probability of 0.5 to fly to get closer to the personal best of a particle randomly chosen from part I, and has probability of 0.5 to fly to get farther away from it). The purpose of this strategy is to keep the particles in part II flying around part I to extend the coverage of the particle population to avoid being trapped into a local optimum. The roles of the two parts in MEPSO are considered originally to be different. Part I is designed to enhance the algorithm's ability of exploitation, while part II is designed to enhance the algorithm's ability of exploration. The two parts work separately, but particles in these two parts are also interrelated. On the one hand, the personal best of particles randomly chosen in part I are used to compose the new velocities of the particles in part II, and then influence their relative position with respect to particles in part I. On the other hand, the best solution found by part II can be the global attractor of part I (if it is also the best of the entire swarm), which will guide the part I fly to the new best (maybe the changed optimum). The overall algorithm is summarized as follows.

Step1: Randomize the positions and velocities of all the particles in the search space. Set all the attractors to a randomized particle position. Divide all the particles into two parts. Set part I's attractor to be the best position of the entire swarm.

Step2: Evaluate the randomly chosen

Step3: IF the new value is different from the last iteration, re-evaluate the function values at each particle attractor in part I.

Step4: Re-randomize each particle in part II.

Step5: Update part I's attractor.

Step6: FOR each particle i in part I IF random number < P_{ls} THEN, the random number within (0, 1), Apply Eq. (6) to renew the velocity, perform a local search

ELSE, Apply Eq. (3) to renew the velocity.

Step7: FOR each particle j in part II, Randomly choose a particle a from part I. Apply Eq. (7) to renew the velocity.//including operator of differential mutation

Step8: FOR each particle j both in part I and part II Apply Eq. (4) to renew the position.

Step9: Evaluate function at updated position. IF new value better than particle attractor value THEN, Particle attractor j: position and value of particle

Step10: IF new value better than part I's attractor value THEN, Part I's attractor: = position and value of particle

Step11: UNTIL number of function evaluations performed > max

There are mainly two parameters that should be set before the execution of the algorithm: the proportion of part I to the whole population P_{one}, the probability P_{ls} of performing a Gaussian local search. The first parameter may be used to control the contribution of part I and part II to the whole performance of the algorithm, and therefore, has an influence on the trade-off between the algorithm's performance on convergence and diversity maintenance. The second parameter may be used to control the proportion of particles in part I that perform the Gaussian local search other than the conventional strategy of PSO, and thus has an influence on the trade-off between the algorithm's performance on local search and global search.

4 EXPERIMENTAL RESULTS

The execution of extrusion in this study results in compressive stresses and the fracturing of the hard ceramic particles within the deforming composites. **Figure 3** shows the light microphotographs of extruded volume fraction of Al6061–12.5 % B_4C composites. It should be noted that a combination of the semi-solid technique and extrusion in the fabrication of these composites leads to a reasonably uniform distribution of particles in the matrix and avoids clustering or agglomeration of the reinforcing phase. The presence of segregated B_4C particles can be easily recognized in the case of uncoated composites. Coated B_4C particles appear more homogeneous throughout the extruded matrix alloy. It is assumed that TiB_2 coating improves the wetting kinetics in the liquid aluminum, which results in a uniform distribution of the coated B_4C particles.[22–26]

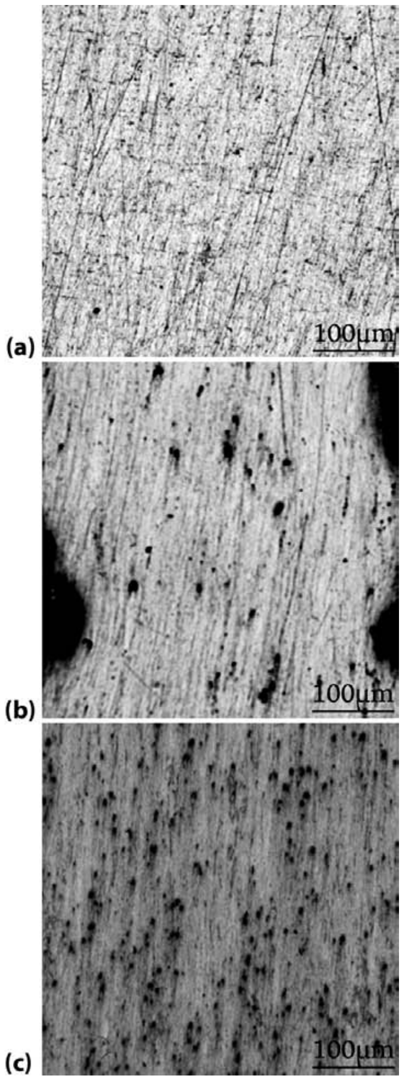

Figure 3: The light micrographs: a) unreinforced Al6061, b) Al6061-12.5 % uncoated B_4C, c) Al6061–12.5 % coated B_4C
Slika 3: Mikrostruktura: a) neojačan Al6061, b) Al6061–12,5 % neoplaščen B_4C, c) Al6061–12,5 % oplaščen B_4C

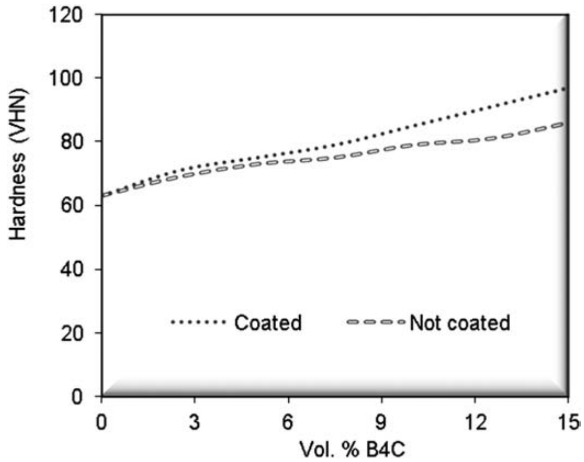

Figure 4: The influence of B_4C reinforcement on the hardness of the composites
Slika 4: Vpliv dodatka delcev B_4C na trdoto kompozita

The variation in the hardness of the extruded Al6061 alloy and its composites with the volume fraction of B_4C particles is presented in **Figure 4**. It is observed that the hardness of the composite samples increases with an increase in the B_4C content. However, coated composites exhibit a higher hardness compared to the uncoated ones. **Figures 5** and **6** show the results of the tensile strength in the extruded Al6061 alloy and its composites. In general, it is noted that both the yield strength and the ultimate tensile strength increase with the increasing the volume fraction of the incorporated B_4C particles for all the materials studied. The improvement in the tensile strength of the composites is the outcome of a higher dislocation density and plastic constraint in the matrix. The strain-hardening of the composites is expected to be influenced by the dislocation density, the dislocation-to-dislocation interaction and the constraint of the plastic

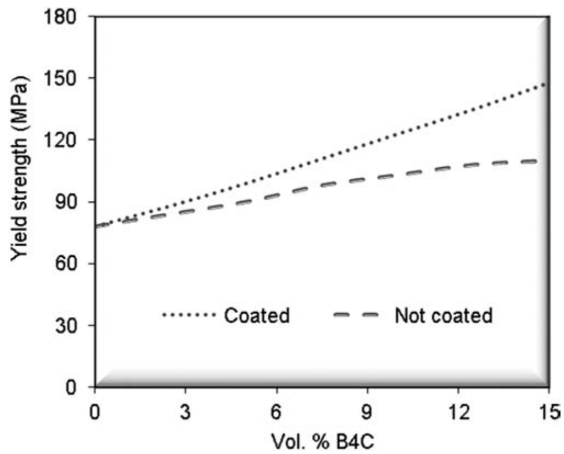

Figure 5: The influence of B_4C reinforcement on the yield strength of the composites
Slika 5: Vpliv dodatka delcev B_4C na mejo plastičnosti kompozita

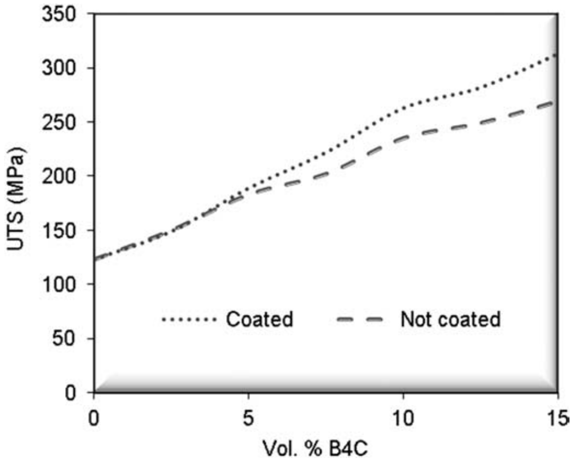

Figure 6: The influence of B_4C reinforcement on the UTS of the composites
Slika 6: Vpliv dodatka delcev B_4C na natezno trdnost kompozita

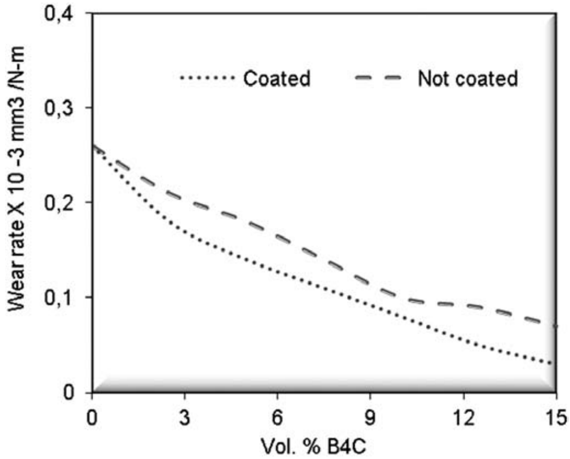

Figure 8: The influence of B_4C reinforcement on the wear rates of the composites
Slika 8: Vpliv delcev B_4C na hitrost obrabe kompozita

flow due to the resistance offered by the particles. The matrix could flow only with the movement of the B_4C particles or over the particles during plastic deformation.[31–39]

Given the fact that the maximum solubility of B and C inside Al melt is not high, these two elements dissolute and saturate the melt rapidly in the case of uncoated composites, which leads to the nucleation of other products on impurity seeds or at the B_4C surface from the supersaturated melt. However, in the case of coated composites, most of the initial B_4C and Al remain unreacted, indicating the phases are conserved for desirable applications. The XRD pattern of the coated B_4C-reinforced composites is displayed in **Figure 7**. It can be seen that B_4C, TiB_2 and aluminum are present and no other reaction products are formed in the system. It is interesting to note that the rate of improvement in the yield strength and the ultimate tensile strength of the coated reinforced composites is higher when compared with the uncoated samples, which can be attributed to a number of reasons, including the absence of interfacial reactions in coated reinforced composites. In addition, a more uniform distribution of particles and a smaller

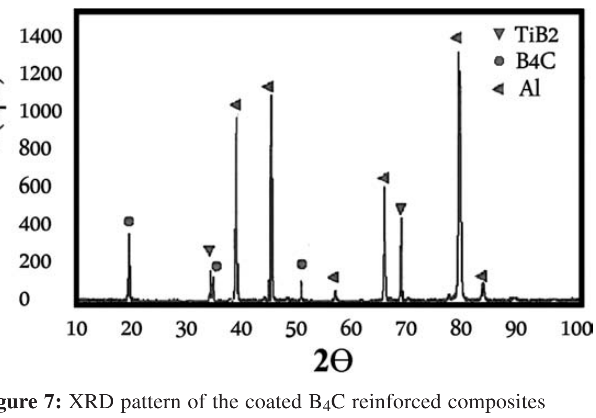

Figure 7: XRD pattern of the coated B_4C reinforced composites
Slika 7: Rentgenska difrakcija kompozita z oplaščenimi delci B_4C

inter-particle distance in the case of coated composites cause the matrix to become considerably constrained and this results in a higher degree of improvement in flow stress and UTS.

Figure 8 shows the influence of B_4C reinforcement on the wear rates of the Al6061 alloy. It is clear that the wear rates of the Al6061 alloy decrease with the addition of the B_4C reinforcement. This improvement in the wear resistance of the composites can be attributed to the formation of mechanically mixed layers (MML) consisting of oxides of iron and aluminium during the sliding of composites on hard steel surfaces. It should be noted that coated composites exhibit a higher wear resistance than the Al6061 matrix alloy and the uncoated composites. The higher hardness, the uniform distribution of particles through the matrix alloy and the strong interfacial bond that exists between the matrix and the reinforcement increase the load-bearing capacity and minimize the matrix contact area in case of the coated B_4C reinforced composite. **Figure 9** shows the worn surfaces of the unreinforced Al alloy and the composites. Extensive cracking and shearing are observed on the worn surfaces of the Al alloy. SEM micrographs indicate wider grooves and a greater extent of the damaged area on the worn surfaces of the uncoated samples, compared to the coated ones.

5 MODELING RESULTS

For MEPSO, the parameters used in Eqs. (4) and (7) are: $w = 0.25$, $c_1 = c_2 = 2.0$. Unless stated otherwise, the probability of a Gaussian local search P_{ls} is set to be 0.15, and the coefficient c_3 in Eq. (6) is set to be 0.3. The proportion of part I $P_{one} = 0.3$, and the proportion of part II $(1 - P_{one}) = 0.7$, i.e., the ratio of part I and part II was 3 : 7. When the dimensionality of the solution space increases, the problem becomes more and more difficult due to the increase in the number of local optima; therefore, the algorithms are more likely to be trapped into the local optimum. As can be seen, MEPSO has the

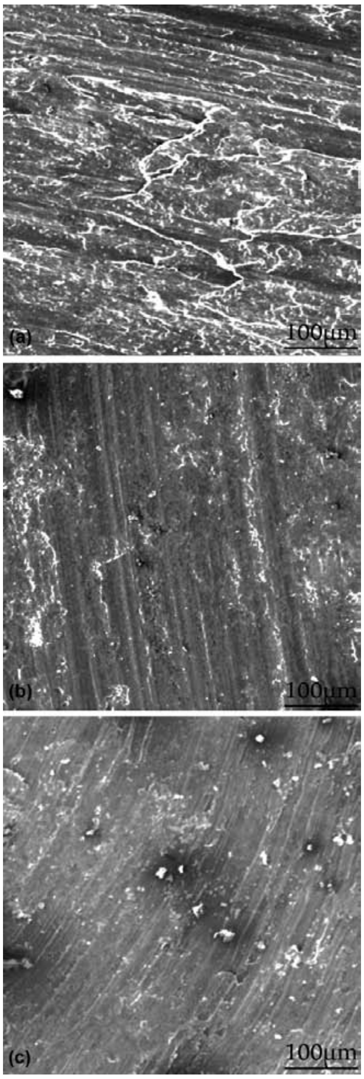

Figure 9: Worn surfaces of the unreinforced Al alloy and the composites: a) unreinforced Al6061 alloy, b) Al6061–10 % uncoated B_4C, c) Al6061-10 % coated B_4C

Slika 9: Obrabljena površina neojačane Al-zlitine in kompozitov: a) neojačana zlitina Al6061, b) Al6061–10 % neoplaščen B_4C, c) Al6061 –10 % oplaščen B_4C

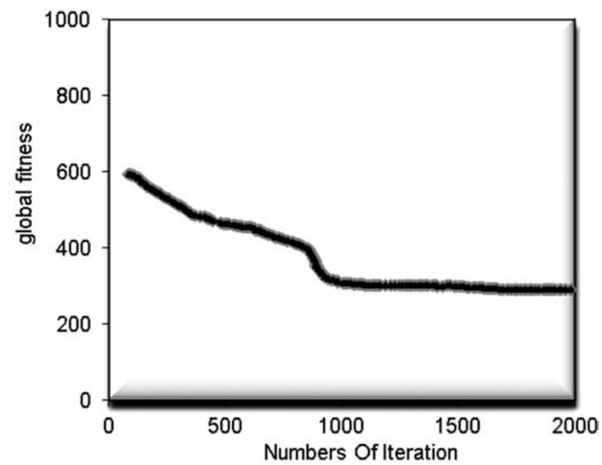

Figure 10: The effect of iteration number on the global fitness

Slika 10: Vpliv števila ponovitev na globalno zmogljivost modela

best performance in all the dimensionality conditions, and the offline error gap between the MEPSO and other algorithms becomes larger and larger as the dimensionality increases. In the following experiments, for MEPSO we use the method of re-evaluating five randomly chosen "sentry" particles to detect the change of the environments. When the changes have been detected, we re-evaluate each particle's best position and current position in part I, and then update each memory with the better position. The re-randomization mechanism is applied to all the particles in part II after the environment changes. The methods of detecting changes and handling outdated memories of the compared algorithms are the same as that adopted in[1–5]. It is clear that MEPSO copes well with both unimodal and multimodal dynamic problems. A possible reason may stem from the ensemble of multiple strategies: from the experimental analysis, it can be observed that the mechanisms used in part I have a good effect on the convergence performance of the algorithm; while the mechanisms adopted in part II can extend the coverage of the particle population to avoid being trapped into the local optimum, and to enhance the ability of catching up with the changing optimum in dynamic multimodal environments. **Figure 10** shows the effect of iteration number on the global fitness of the developed model. The numbers of the iteration were selected to be 2000.

The value of P_{ls} varies from 0.0 to 0.9. Good results are achieved for $0.1 = P_{ls} = 0.2$ in various severity and multimodal environments. When $P_{ls} > 0.4$, the performance gets rapidly worse as the value of P_{ls} increases. It is obvious that when the value of P_{ls} is set to be close to or equal to 0, the results are getting much worse than those attained for $0.1 = P_{ls} = 0.2$. From the experimental results it is clear that, it is effective to perform a proper local search for the particles in part I. The value of P_{ls} must not be too large or too small, i.e., $0.1 = P_{ls} = 0.2$ is the best choice. What is more, the same conclusion can be drawn for various dynamic problem settings; in other words, the performance of MEPSO is rather robust to various dynamic problems with the parameter P_{ls} setting range from 0.1 to 0.2. The final optimized parameters are 617.48 s stirring time, 644.26 r/min speed of stirrer, 31.43 μm particle size of B_4C, 11.53 % volume fractions of B_4C, 87.21 VHN hardness, 0.43 % porosity, 277.21 MPa UTS, 133.57 MPa yield strength, 0.06 10^{-3} $mm^3/(N\ m)$ wear rates and 5.73 % elongation. The results show that the novel technique implemented in this investigation has an acceptable performance. Therefore, this work shows the usefulness of an intelligent way to predict the performance of aluminum matrix composites using Multi-strategy ensemble particle-swarm optimization.

6 CONCLUSION

In MEPSO, the whole population of particles is divided into two parts: part I works as a standard PSO enhanced with a Gaussian local search strategy, part II works as a patrol team around part I to extend the search area of the algorithm, and to catch up with the moving optimum. It is concluded that extrusion of the fabricated composites helps to reduce the B_4C particles size in both TiB_2 coated and uncoated B_4C reinforced composites. This can be attributed to fact that, the execution of the extrusion results in compressive stresses and therefore fracturing of the hard ceramic particles within the deforming composites. It should be noted that the particle distribution in the coated composites is much more uniform than the uncoated ones. The strong interfacial bond that exists between the matrix and the reinforcement in the case of coated B_4C reinforced composites contributes significantly to the improved wear resistance by increasing the load-transfer efficiency between the matrix and the reinforcement. Furthermore, a poor interfacial bond between the hard B_4C reinforcement and the soft matrix alloy will lead to the three-body abrasive wear phenomenon.

7 REFERENCES

[1] J. J. Liang, A. K. Qin, P. N. Suganthan, S. Baskar, IEEE Transactions on Evolutionary Computation, 10 (**2006**), 281–295

[2] M. O. Shabani, A. Mazahery, Mater. Tehnol., 46 (**2012**) 6, 613–619

[3] J. Kennedy, R. C. Eberhart, Particle swarm optimization, In: Proceedings of the IEEE International Conference on Neural Networks, vol. IV, Perth, Australia, 1995, 1942–1948

[4] A. Mazahery, M. O. Shabani, JOM, 66 (**2014**) 5, 726–738

[5] A. Mazahery, M. O. Shabani, Powder Technology, 225 (**2012**), 101–106

[6] A. A. Tofigh, M. O. Shabani, Ceramics International, 39 (**2013**), 7483–7490

[7] M. O. Shabani, A. Mazahery, Appl. Math. Model., 36 (**2012**), 5455–5465

[8] D. Beasley, D. R. Bull, R. R. Martin, Evolutionary Comput., 1 (**1993**) 2, 101–125

[9] R. Brits, Niching Strategies for Particle Swarm Optimization, Master's thesis, Department of Computer Science, University of Pretoria, Pretoria, South Africa, 2002

[10] M. O. Shabani, A. Mazahery, Metall. Mater. Trans. A, 43 (**2012**), 2158–2165

[11] A. Mazahery, M. O. Shabani, Powder Technology, 249 (**2013**), 530–535

[12] A. Mazahery, M. O. Shabani, JOM, 64 (**2012**) 2, 323–329

[13] J. Kennedy, R. C. Eberhart, Swarm Intelligence, Morgan Kaufman, 2001

[14] J. Kennedy, R. Mendes, Population structure and particle swarm performance, In: Proceedings of the IEEE World Congress on Evolutionary Computation, Honolulu, Hawaii, 2002, 1671–1676

[15] F. van den Bergh, A. P. Engelbrecht, Information Science, 176 (**2006**) 8, 937–971

[16] C. Wang, Z. Zhong, E. Jiaqiang, Powder Technology, 219 (**2012**), 20–28

[17] R. Bauri, M. K. Surappa, Journal of Material Processing Technology, 209 (**2009**), 2077–2084

[18] M. O. Shabani, A. Mazahery, Ceram. Int., 39 (**2013**), 5271–5279

[19] J. Hashim, L. Looney, M. S. J. Hashmi, J. Mater. Process. Technol., 123 (**2002**), 251–257

[20] A. Mazahery, M. O. Shabani, Powder Technology, 217 (**2012**), 558–565

[21] V. Kevorkijan, R. Hexemer, Kovine zlitine tehnologije, 32 (**1998**) 5, 397–402

[22] M. O. Shabani, A. Mazahery, Mater. Tehnol., 46 (**2012**) 2, 109–113

[23] K. S. Vinoth, R. Subramanian, Mater. Tehnol., 46 (**2012**) 5, 497–501

[24] A. Mazahery, M. O. Shabani, Composites: Part B, 43 (**2012**), 1302–1308

[25] S. K. Rhee, J. Am. Ceram. Soc., 53 (**1970**), 386

[26] M. O. Shabani, A. Mazahery, Indian Journal of Engineering & Materials Sciences, 19 (**2012**), 129–134

[27] M. Razavi, M. R. Rahimipour, R. Kaboli, Journal of Alloys and Compounds, 460 (**2008**), 694–698

[28] M. Demirel, M. Muratoglu, Mater. Tehnol., 45 (**2011**) 5, 401–406

[29] M. O. Shabani, A. Mazahery, Trans Indian Inst Met., 65 (**2012**) 1, 77–83

[30] M. Gupta, L. Lu, S. E. Ang, J. Mater. Sci., 32 (**1997**), 1261–1267

[31] V. Kevorkijan, B. Šuštaršič, M. Torkar, G. Chiarmetta, Kovine zlitine tehnologije, 32 (**1998**) 6, 539–543

[32] A. Mazahery, M. O. Shabani, Tribology Transactions, 56 (**2013**), 342–348

[33] C. J. Quaak, W. H. Kool, Mater. Sci. Eng. A, 188 (**1994**), 277–282

[34] M. O. Shabani, A. Mazahery, Archives of Metallurgy and Materials, 56 (**2011**) 3, 671–675

[35] A. J. Asthana, Journal of Material Science and Engineering, 35 (**1998**), 1959–1980

[36] C. A. Leon, R. L. Drew, J. of Mater. Sci., 35 (**2000**), 4763–4768

[37] A. Mazahery, M. O. Shabani, Journal of Materials Engineering and Performance, 21 (**2012**) 2, 247–252

[38] L. M. Tham, M. Gupta, L. Cheng, Acta Materialia, 49 (**2001**), 3243–3253

[39] M. O. Shabani, A. Mazahery, Composites: Part B, 45 (**2013**), 185–191

[40] A. A. Tofigh, M. R. Rahimipour, M. O. Shabani, M. Alizadeh, F. Heydari, A. Mazahery, M. Razavi, Journal of Manufacturing Processes, 15 (**2013**), 518–523

[41] S. F. Moustafa, S. A. Badry, A. M. Sanad, B. Kieback, Wear, 253 (**2002**), 699–710

[42] A. Mazahery, M. O. Shabani, Russian Metallurgy (Metally), 7 (**2011**), 699–707

[43] U. Cocen, K. Onel, Composite Science Technology, 62 (**2002**), 275–282

[44] M. McKimpson, T. Scott, Mater. Sci. Eng., 107 (**1989**), 93–106

[45] A. Mazahery, M. O. Shabani, Trans Indian Inst Met., 65 (**2012**) 2, 145–154

[46] V. K. Varma, S. V. Kamath, V. V. Kutumabarao, Material Science and Technology, 17 (**2000**), 921–936

[47] M. O. Shabani, A. Mazahery, Powder Technology, 249 (**2013**), 77–81

[48] M. O. Shabani, A. Mazahery, JOM, 63 (**2011**) 8, 132–136

[49] Y. G. Petalas, C. G. Antonopoulos, T. C. Bountis, M. Vrahatis, Phys. Lett. A, 373 (**2009**), 334–341

[50] A. Mazahery, M. O. Shabani, Metall and Mat Trans A, 43 (**2012**), 5279–5285

[51] C. H. Wu, N. Dong, W. H. Ip, C. Y. Chen, K. L. Yung, Z. Q. Chen, Lecture Notes in Comput. Sci., 6024 (**2010**), 302–311

[52] M. O. Shabani, M. Alizadeh, A. Mazahery, Fatigue Fract Engng Mater Struct., 34 (**2011**), 1035–1040

[53] S. Z. Zhao, P. N. Suganthan, Engineering Optimization, 43 (**2011**) 1, 1–17

[54] K. Elsayed, C. Lacor, Powder Technology, 217 (**2012**), 84–99